

The **next generation** GBCA  
from Guerbet is here

Explore new possibilities >

Guerbet | 

© Guerbet 2024 GUOB220151-A

# AJNR

## **Interobserver Reliability on Intravoxel Incoherent Motion Imaging in Patients with Acute Ischemic Stroke**

K. Yamashita, R. Kamei, H. Sugimori, T. Kuwashiro, S.  
Tokunaga, K. Kawamata, K. Furuya, S. Harada, J. Maehara,  
Y. Okada and T. Noguchi

This information is current as  
of September 19, 2024.

*AJNR Am J Neuroradiol* 2022, 43 (5) 696-700  
doi: <https://doi.org/10.3174/ajnr.A7486>  
<http://www.ajnr.org/content/43/5/696>

# Interobserver Reliability on Intravoxel Incoherent Motion Imaging in Patients with Acute Ischemic Stroke

 K. Yamashita,  R. Kamei,  H. Sugimori,  T. Kuwashiro,  S. Tokunaga,  K. Kawamata,  K. Furuya,  S. Harada,  J. Maehara,  Y. Okada, and  T. Noguchi



## ABSTRACT

**BACKGROUND AND PURPOSE:** Noninvasive perfusion-weighted imaging with short scanning time could be advantageous in order to determine presumed penumbral regions and subsequent treatment strategy for acute ischemic stroke (AIS). Our aim was to evaluate interobserver agreement and the clinical utility of intravoxel incoherent motion MR imaging in patients with acute ischemic stroke.

**MATERIALS AND METHODS:** We retrospectively studied 29 patients with AIS (17 men, 12 women; mean age, 75.2 [SD, 12.0] years; median, 77 years). Each patient underwent intravoxel incoherent motion MR imaging using a 1.5T MR imaging scanner. Diffusion-sensitizing gradients were applied sequentially in the x, y, and z directions with 6 different b-values (0, 50, 100, 150, 200, and 1000 seconds/mm<sup>2</sup>). From the intravoxel incoherent motion MR imaging data, diffusion coefficient, perfusion fraction, and pseudodiffusion coefficient maps were obtained using a 2-step fitting algorithm based on the Levenberg-Marquardt method. The presence of decreases in the intravoxel incoherent motion perfusion fraction and pseudodiffusion coefficient values compared with the contralateral normal-appearing brain was graded on a 2-point scale by 2 independent neuroradiologists. Interobserver agreement on the rating scale was evaluated using the  $\kappa$  statistic. Clinical characteristics of patients with a nondecreased intravoxel incoherent motion perfusion fraction and/or pseudodiffusion coefficient rated by the 2 observers were also assessed.

**RESULTS:** Interobserver agreement was shown for the intravoxel incoherent motion perfusion fraction ( $\kappa = 0.854$ ) and pseudodiffusion coefficient ( $\kappa = 0.789$ ) maps, which indicated almost perfect and substantial agreement, respectively. Patients with a nondecreased intravoxel incoherent motion perfusion fraction tended to show recanalization of the occluded intracranial arteries more frequently than patients with a decreased intravoxel incoherent motion perfusion fraction.

**CONCLUSIONS:** Intravoxel incoherent motion MR imaging could be performed in <1 minute in addition to routine DWI. Intravoxel incoherent motion parameters noninvasively provide feasible, qualitative perfusion-related information for assessing patients with acute ischemic stroke.

**ABBREVIATIONS:** AIS = acute ischemic stroke; D = diffusion coefficient; D\* = pseudo-diffusion coefficient; EVT = endovascular thrombectomy; f = perfusion fraction; IVIM = intravoxel incoherent motion

MR imaging is one of the best modalities for diagnosing acute ischemic stroke (AIS) and plays a crucial role in treatment

decisions for procedures such as endovascular thrombectomy (EVT). A multicenter randomized clinical trial (Multicenter Randomized Clinical trial of Endovascular treatment for Acute ischemic stroke in the Netherlands; the MR CLEAN trial) revealed notable benefits from EVT in patients with AIS.<sup>1</sup> Positive results from the Endovascular Therapy Following Imaging Evaluation for Ischemic Stroke 3 (DEFUSE 3)<sup>2</sup> and Clinical Mismatch in the Triage of Wake Up and Late Presenting Strokes Undergoing Neurointervention with Trevo (DAWN) trials<sup>3</sup> have extended the therapeutic windows for AIS.

Findings from DWI are important for determining ischemic cores and have been included for assessing infarct volume in randomized clinical trials such as DEFUSE 3 and DAWN.<sup>2,3</sup> CT perfusion imaging provides useful information to identify presumed

Received November 10, 2021; accepted after revision February 11, 2022.

From the Departments of Radiology (K.Y., R.K., K.F., S.H., J.M., T.N.), Cerebrovascular Medicine and Neurology (H.S., T.K., Y.O.), Neuroendovascular Therapy (S.T.), Clinical Research Institute, and Medical Technology (K.K.), Division of Radiology, National Hospital Organization Kyushu Medical Center, Fukuoka, Japan.

This work was supported by Nishikawa Medical Foundation, and the Japan Society for the Promotion of Science (JSPS) KAKENHI Grant Number 22K07657.

Please address correspondence to Koji Yamashita, MD, PhD, Department of Radiology, Clinical Research Institute, National Hospital Organization Kyushu Medical Center, 1-8-1 Jigyohama, Chuo-ku, Fukuoka 810-0065 Japan; e-mail: yamakou@radiol.med.kyushu-u.ac.jp

 Indicates open access to non-subscribers at [www.ajnr.org](http://www.ajnr.org)

<http://dx.doi.org/10.3174/ajnr.A7486>

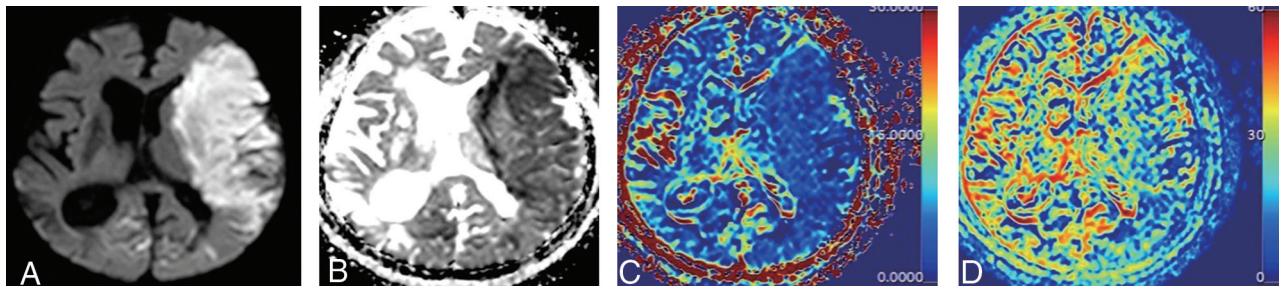


**FIG 1.** Representative DWI with a b-value of 1000 s/mm<sup>2</sup> (A), IVIM D (B), f (C), and D\* (D) maps obtained using a 2-step algorithm. A 90-year-old woman with AIS. IVIM f and D\* are expressed in units of percentage and  $\times 10^{-3}$  mm<sup>2</sup>/s, respectively. Interobserver agreement is shown for IVIM f ( $\kappa = 0.854$ ;  $P < .001$ ) and D\* ( $\kappa = 0.789$ ;  $P < .001$ ) using the 2-step algorithm, which indicated almost perfect and substantial agreement, respectively.

penumbral regions and has a large influence on decision-making for EVT. On the other hand, CT perfusion depends on factors such as motion, the time-density curve, determination of arterial input functions, and so forth.<sup>4</sup> Technical pitfalls including core volume measurement error, misclassification of ischemic penumbra, and stroke mimics (seizure, migraines, and posterior reversible leukoencephalopathy) are also well-known.<sup>4</sup> Theoretically, perfusion-weighted MR imaging provides less misregistration of lesions that appear hyperintense on DWI than other imaging modalities.

Dynamic susceptibility contrast, dynamic contrast enhancement, arterial spin-labeling, and intravoxel incoherent motion (IVIM) imaging offer perfusion-related parameters. Among these methods, IVIM imaging would provide advantages in terms of noninvasiveness as well as allowing registration with DWI. Le Bihan et al<sup>5</sup> implemented the concept of IVIM MR imaging to separate the signal into diffusivity and microcapillary perfusion components with different exponential decays. IVIM MR imaging allows simultaneous extraction of perfusion and diffusion parameters and is reportedly useful for differentiating high- and low-grade gliomas,<sup>6,7</sup> glioblastomas and lymphomas,<sup>8,9</sup> and pediatric brain tumors.<sup>10</sup> Ideally, a shorter scanning time using a small number of b-values would lead to advantages in reducing the time to subsequent reperfusion therapy. Federau et al<sup>11</sup> reported the feasibility of IVIM MR imaging using 6 b-values for AIS: 0, 50, 100, 150, 200, and 1000 s/mm<sup>2</sup>. However, the interobserver reliability of IVIM MR imaging using these 6 b-values and the clinical characteristics of patients with decreased or nondecreased IVIM parameters have not been well-explored.

The goal of this study was, therefore, to evaluate interobserver agreement and the clinical utility of IVIM MR imaging in patients with AIS.

## MATERIALS AND METHODS

### Subjects

This retrospective study was approved by National Hospital Organization Kyushu Medical Center institutional review board for clinical research. The requirement of obtaining informed consent for study participation was waived due to the retrospective nature of this study. We studied 35 patients with nonlacunar AIS (21 men, 14 women; mean age, 75.6 [SD, 11.6] years; median age, 77 years) between August 2020 and June 2021. All subjects fulfilled the following criteria: MR imaging performed within 7 days

after either symptom onset or last seen well, and patients undergoing IVIM imaging. Six of the 35 patients were excluded from the study due to motion-related image degradation.

### MR Imaging

All images were obtained using a 1.5T MR imaging scanner (Achieva; Philips Healthcare) and an 8-channel head array receiving coil for sensitivity encoding parallel imaging. IVIM imaging was performed using a single-shot spin-echo echo-planar sequence with the following parameters: TR, 3500 ms; TE, 75 ms; flip angle, 90°; NEX, 1; transverse sections, 23; sensitivity encoding factor, 2; section thickness, 5 mm; interslice gap, 1.5 mm; FOV, 220 × 220 mm; matrix, 124 × 105; and imaging time, 1 minute 24 seconds. Diffusion-sensitizing gradients were implemented in 3 orthogonal directions with 6 different b-values (0, 50, 100, 150, 200, and 1000 s/mm<sup>2</sup>). Directional averaging was performed before applying the IVIM model.

### Postprocessing

From the IVIM imaging data, diffusion coefficient (D), perfusion fraction (f), and pseudodiffusion coefficient (D\*) maps were obtained using a 2-step fitting algorithm based on the Levenberg-Marquardt method. The open-source platform ADCmap Plugin (Version 1.8, <http://web.stanford.edu/~bah/software/ADCmap/versions.html>), running OsiriX Lite, Version 8.0.1 (<https://www.osirix-viewer.com>) was applied for the fitting process for DWI data. In short, D values were calculated using a monoexponential signal equation for b-values  $\geq 200$  s/mm<sup>2</sup> in the first step. Subsequently, curve fitting was performed to obtain f and D\* values using all 6 b-values, while the acquired D value was kept fixed.<sup>12</sup>

### Image Evaluation

Representative DWI with  $b=1000$  s/mm<sup>2</sup> and IVIM parameter (D, f, and D\*) maps are shown in Fig 1. IVIM f and D\* values were evaluated and graded on a 2-point scale by 2 independent neuroradiologists. Two observers determined the presence of decreases in f and D\* values compared with the contralateral normal-appearing brain with reference to the hyperintense region on DWI with a b-value of 1000 s/mm<sup>2</sup>.

Second, clinical characteristics of patients with nondecreased IVIM f and/or D\* as rated by the 2 observers were assessed. Specifically, the cause of AIS was classified as cardioembolic,

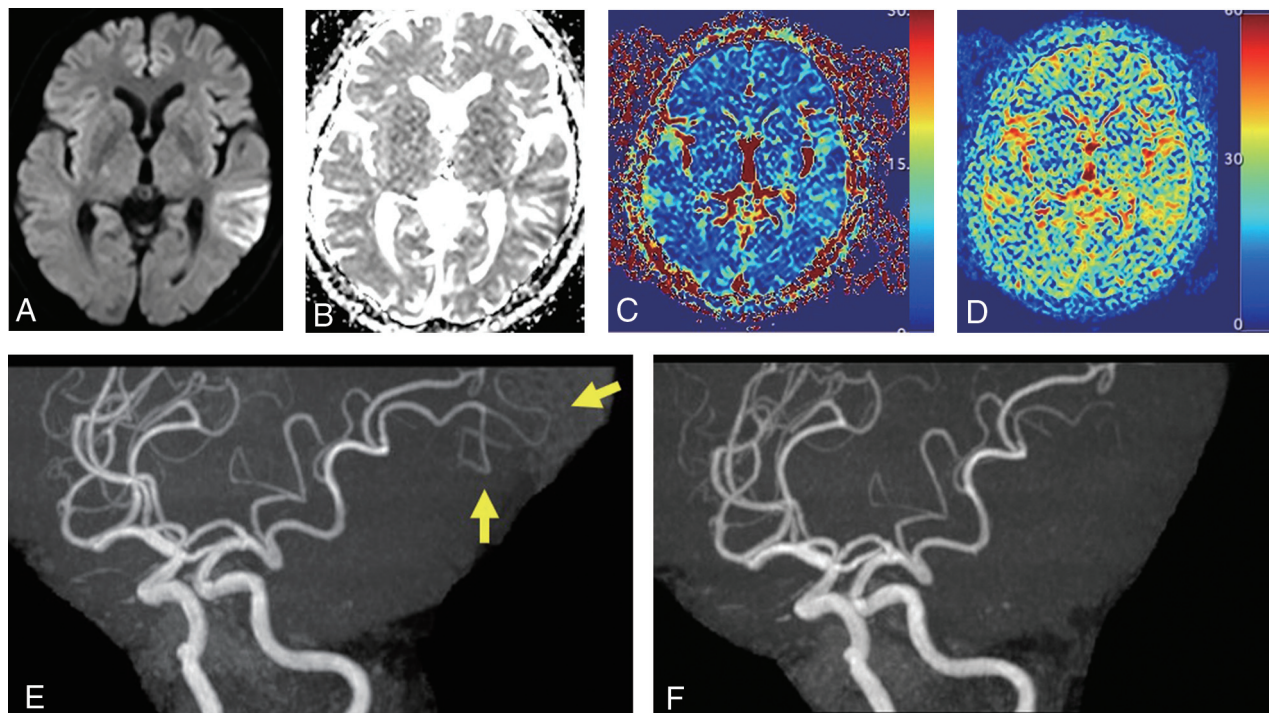


**FIG 2.** A DWI with a b-value of 1000 s/mm<sup>2</sup> (A), IVIM D (B), f (C), D\* (D) maps, and MRA (E) of a 73-year-old man with AIS. MR imaging was performed 7 days after symptom onset. Nondecreased IVIM f and D\* are identified on the f and D\* maps. MR angiography represents spontaneous recanalization of the occluded left distal MCA (E; arrows). MRA performed 33 hours after symptom onset (F) is also shown as a reference.

atherothrombotic, or undetermined. The number of recanalized occluded intracranial arteries was also examined.

Next, a circular ROI (area,  $\geq 10$  mm<sup>2</sup>) was placed, as large as possible, within hyperintense lesions on DWI with a b-value of 1000 s/mm<sup>2</sup> by an experienced neuroradiologist. A mirrored ROI was also drawn in the corresponding contralateral region. ROIs on DWI were copied onto corresponding IVIM parameter (D, f, and D\*) maps to calculate mean values for D, f, and D\* ( $D_{\text{mean}}$ ,  $f_{\text{mean}}$ , and  $D^*_{\text{mean}}$ , respectively).

### Statistical Analyses

Interobserver agreement on the rating of IVIM f and D\* maps was evaluated using  $\kappa$  statistics.  $\kappa$  values for interobserver agreement were evaluated as the following: 0, poor; 0.01–0.20, slight; 0.21–0.40, fair; 0.41–0.60, moderate; 0.61–0.80, substantial; and  $>0.80$ , almost perfect. The difference in the frequency of recanalized occluded intracranial arteries between patients with decreased and nondecreased IVIM f was compared using the Pearson  $\chi^2$  test.

For the correlation between IVIM parameters ( $D_{\text{mean}}$ ,  $f_{\text{mean}}$ , and  $D^*_{\text{mean}}$ ) and time after stroke onset, a simple regression model was used to model trajectories with linear, quadratic, cubic, and logarithmic. The Akaike information criterion was used to determine the best fitting model.

IVIM  $D_{\text{mean}}$ ,  $f_{\text{mean}}$ , and  $D^*_{\text{mean}}$  values were compared between the affected and contralateral unaffected sides using a 2-tailed paired Student *t* test. In all statistical analyses, the level of significance was set at  $P < .05$ . All statistical analyses were performed using R statistical and computing software, Version 3.5.1

(<http://www.r-project.org>), and graphs were plotted on GraphPad Prism, Version 7 (GraphPad Software).

### RESULTS

As a result, a total of 29 patients with AIS (17 men, 12 women; mean age, 75.2 [SD 12.0] years; median age, 77 years) were included in this study. The median time from symptom onset or last seen well to MR imaging was 26 hours (range, 1 hour to 7 days), and the mean NIHSS score at presentation was 6.1 (SD, 7.4). We identified the cause of AIS as cardioembolic in 11 patients, atherothrombotic in 11, and undetermined in 7. A total of 7 cases showed recanalization of occluded intracranial arteries based on MR angiography.

#### Interobserver Agreement on the Rating of IVIM f and D\* Maps

Interobserver agreement was shown for IVIM f ( $\kappa = 0.854$ ,  $P < .001$ ) and D\* ( $\kappa = 0.789$ ,  $P < .001$ ), which indicated almost perfect and substantial agreement, respectively. Figure 1 shows representative IVIM f and D\* maps obtained using the 2-step fitting algorithm.

#### Clinical Characteristics of Patients with Nondecreased IVIM f and/or D\*

The 12 patients with nondecreased IVIM f as rated by observers showed recanalization of occluded intracranial arteries more frequently ( $n = 6$ ; 6/12, 50%) than the 17 patients with decreased IVIM f (1/17, 5.9%;  $P < .05$ ). Patients with nondecreased IVIM D\* showed a trend similar to that in those with nondecreased

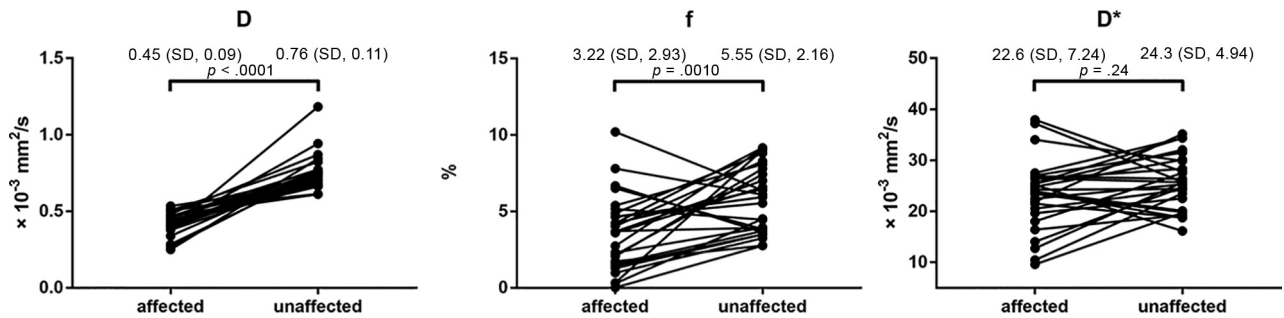


**FIG 3.** Plots of  $D_{\text{mean}}$  (A),  $f_{\text{mean}}$  (B), and  $D^*_{\text{mean}}$  (C) on both the affected and contralateral unaffected sides. The  $D_{\text{mean}}$  and  $f_{\text{mean}}$  values were lower on the affected side (mean  $D_{\text{mean}} = 0.45$  [SD, 0.09]  $\times 10^{-3}$   $\text{mm}^2/\text{s}$ ; mean  $f_{\text{mean}} = 3.22\%$  [SD, 2.93%]) than on the contralateral unaffected side (mean  $D_{\text{mean}} = 0.76$  [SD, 0.11]  $\times 10^{-3}$   $\text{mm}^2/\text{s}$ ,  $P < .0001$ ; mean  $f_{\text{mean}} = 5.55\%$  [SD, 2.16%],  $P = .0010$ ). No statistical difference in mean  $D^*_{\text{mean}}$  was evident between the affected side (22.6 [SD, 7.24]  $\times 10^{-3}$   $\text{mm}^2/\text{s}$ ) and the contralateral unaffected side (24.3 [SD, 4.94]  $\times 10^{-3}$   $\text{mm}^2/\text{s}$ ;  $P = .24$ ).

IVIM  $f$ . Figure 2 shows the case of presumed spontaneous recanalization of an occluded MCA after AIS.

### Correlation between IVIM Parameters and Time after Stroke Onset

The numbers in parentheses represent adjusted  $R^2$  and  $P$  values using the best fitting model based on the Akaike information criterion. No statistical correlation was noted among IVIM  $D_{\text{mean}}$  (0.096, .10),  $f_{\text{mean}}$  (0.16, .06), and  $D^*_{\text{mean}}$  (−0.017, .47) in the presumed ischemic core and time after stroke onset.

### $D_{\text{mean}}$ , $f_{\text{mean}}$ , and $D^*_{\text{mean}}$ on Affected and Contralateral Unaffected Sides

Figure 3 shows plots of  $D_{\text{mean}}$ ,  $f_{\text{mean}}$ , and  $D^*_{\text{mean}}$  for both affected and contralateral unaffected sides. Mean  $D_{\text{mean}}$  and  $f_{\text{mean}}$  values were lower on the affected side (mean  $D_{\text{mean}} = 0.45$  [SD, 0.09]  $\times 10^{-3}$   $\text{mm}^2/\text{s}$ ; mean  $f_{\text{mean}} = 3.22\%$  [SD, 2.93%]) than on the contralateral unaffected side (mean  $D_{\text{mean}} = 0.76$  [SD, 0.11]  $\times 10^{-3}$   $\text{mm}^2/\text{s}$ ,  $P < .0001$ ; mean  $f_{\text{mean}} = 5.55 \pm 2.16\%$ ,  $P = .001$ ). No statistical difference in mean  $D^*_{\text{mean}}$  was evident between the affected side (22.6 [SD, 7.24]  $\times 10^{-3}$   $\text{mm}^2/\text{s}$ ) and the contralateral unaffected side (24.3 [SD, 4.94]  $\times 10^{-3}$   $\text{mm}^2/\text{s}$ ;  $P = .24$ ).

## DISCUSSION

IVIM  $f$  and  $D^*$  using the 2-step fitting algorithm provided the  $\chi$  values of 0.854 and 0.789, respectively, which demonstrated high interobserver agreement and feasible indicators for assessing patients with AIS. Patients with nondecreased IVIM  $f$  and  $D^*$  after AIS had a higher rate of the recanalization of occluded intracranial arteries in this study. IVIM MR imaging with its scanning time of <1 minute in addition to routine DWI with  $b$ -values of 0 and 1000  $\text{s}/\text{mm}^2$  offers a choice of noninvasive perfusion-weighted imaging for patients with suspected AIS.

In the present study, patients with nondecreased IVIM  $f$  and  $D^*$  as rated by the observers showed recanalization of occluded intracranial arteries more frequently than with decreased IVIM  $f$  and  $D^*$ . Padroni et al<sup>13</sup> identified relative CBV as a strong indicator of recanalization status. MTT reportedly offers a valuable tool for assessing patients with AIS who may benefit from EVT.<sup>14</sup> Our results are in line with the findings from previous studies. In addition, Eilaghi et al<sup>15</sup> indicated that reperfusion indices for CBF, CBV, MTT, and time to maximum were more highly

associated with good clinical outcome than recanalization status. Validation using longitudinal data comprising values both before and after recanalization of occluded intracranial arteries would strengthen our results and represents the next step in our research.

Minimizing misinterpretation of IVIM parameter maps for clinical use is important. Almost perfect interobserver agreement was seen for IVIM  $f$ , and substantial agreement, for IVIM  $D^*$  as rated by the 2 observers in this study. A total of 6  $b$ -values (0, 50, 100, 150, 200, and 1000  $\text{s}/\text{mm}^2$ ) have been accepted as the reference standard for IVIM MR imaging when assessing AIS.<sup>11,16</sup> More complex models would provide better results, while sophisticated models may cause the problem of overfitting due to data variations contaminated by noise and motion.<sup>17</sup> IVIM parameter maps allow more accurate imaging evaluation with hyperintense lesions on DWI over other perfusion-weighted imaging such as dynamic susceptibility contrast, dynamic contrast enhancement, or arterial spin-labeling in terms of misregistration. MR perfusion-weighted imaging using IVIM is reportedly useful in patients with stroke with large-vessel occlusion.<sup>11</sup> IVIM parameter maps obtained from the 2-step fitting algorithm look less complicated with lower image noise than biexponential models, though which method is better for assessing AIS remains uncertain.

$D_{\text{mean}}$  and  $f_{\text{mean}}$  values were lower on the affected side than on the contralateral unaffected side. IVIM  $f$  is related to blood volume.<sup>11,18</sup> Our result is consistent with previous literature using MR imaging and PET.<sup>19,20</sup> In contrast, we observed no statistical differences in  $D^*_{\text{mean}}$  values between the affected and contralateral unaffected sides. IVIM  $D^*$  is related to blood speed but fluctuates during the cardiac cycle, in contrast to the  $f$  and  $D$  values.<sup>21</sup> IVIM  $D^*$ , thus, should be evaluated carefully along with other parameters.

In the present study, no correlation was observed between IVIM parameters in the presumed ischemic core and time after stroke onset. Fiebach et al<sup>22</sup> reported the time course for the ADC in the ischemic core. Our results were not consistent with that research, possibly due to differences in the distribution of stroke subtypes and recanalization of occluded intracranial arteries.

Our study had several limitations. First, the present study comprised a small number of cases with various stroke subtypes and elapsed time from stroke onset. It is important to identify the

at-risk-but-viable penumbral tissue in the setting of AIS. Decreased IVIM  $f$  was presumed the infarct core with AIS<sup>23</sup> or a penumbral lesion in hyperacute brain stroke.<sup>11</sup> Further validation studies with larger sample sizes are needed. Second, this study was retrospective in nature, and selection bias due to nonrandom selection may have occurred. Third, a minimum of 6 directions should be acquired in the DTI framework, though it might take too long in the context of AIS.<sup>24</sup> Last, about half of the subjects had already undergone administration of intravenous recombinant tPA or endovascular treatment before MR imaging. Thus, further validation studies using longitudinal data are needed in the future. Nevertheless, we believe our results shed light on the availability of IVIM parameters in routine clinical practice.

## CONCLUSIONS

IVIM MR imaging noninvasively provides feasible qualitative information in assessing patients with AIS.

Disclosure forms provided by the authors are available with the full text and PDF of this article at [www.ajnr.org](http://www.ajnr.org).

## REFERENCES

- Berkhemer OA, Fransen PSS, Beumer D, et al; MR CLEAN Investigators. A randomized trial of intraarterial treatment for acute ischemic stroke. *N Engl J Med* 2015;372:11–20 [CrossRef Medline](#)
- Albers GW, Marks MP, Kemp S, et al. Thrombectomy for stroke at 6 to 16 hours with selection by perfusion imaging. *N Engl J Med* 2018;378:708–18 [CrossRef Medline](#)
- Nogueira RG, Jadhav AP, Haussen DC, et al. Thrombectomy 6 to 24 hours after stroke with a mismatch between deficit and infarct. *N Engl J Med* 2018;378:11–21 [CrossRef Medline](#)
- Vagal A, Wintermark M, Nael K, et al. Automated CT perfusion imaging for acute ischemic stroke: pearls and pitfalls for real-world use. *Neurology* 2019;93:888–98 [CrossRef Medline](#)
- Le Bihan D, Breton E, Lallemand D, et al. MR imaging of intravoxel incoherent motions: application to diffusion and perfusion in neurologic disorders. *Radiology* 1986;161:401–07 [CrossRef Medline](#)
- Federau C, Meuli R, O'Brien K, et al. Perfusion measurement in brain gliomas with intravoxel incoherent motion MRI. *AJNR Am J Neuroradiol* 2014;35:256–62 [CrossRef Medline](#)
- Togao O, Hiwatashi A, Yamashita K, et al. Differentiation of high-grade and low-grade diffuse gliomas by intravoxel incoherent motion MR imaging. *Neuro Oncol* 2016;18:132–41 [CrossRef Medline](#)
- Yamashita K, Hiwatashi A, Togao O, et al. Diagnostic utility of intravoxel incoherent motion MR imaging in differentiating primary central nervous system lymphoma from glioblastoma multiforme. *J Magn Reson Imaging* 2016;44:1256–61 [CrossRef Medline](#)
- Suh CH, Kim HS, Jung SC, et al. MRI as a diagnostic biomarker for differentiating primary central nervous system lymphoma from glioblastoma: a systematic review and meta-analysis. *J Magn Reson Imaging* 2019;50:560–72 [CrossRef Medline](#)
- Kikuchi K, Hiwatashi A, Togao O, et al. Intravoxel incoherent motion MR imaging of pediatric intracranial tumors: correlation with histology and diagnostic utility. *AJNR Am J Neuroradiol* 2019;40:878–84 [CrossRef Medline](#)
- Federau C, Wintermark M, Christensen S, et al. Collateral blood flow measurement with intravoxel incoherent motion perfusion imaging in hyperacute brain stroke. *Neurology* 2019;92:e2462–71 [CrossRef Medline](#)
- Federau C, Maeder P, O'Brien K, et al. Quantitative measurement of brain perfusion with intravoxel incoherent motion MR imaging. *Radiology* 2012;265:874–81 [CrossRef Medline](#)
- Padroni M, Bernardoni A, Tamborino C, et al. Cerebral blood volume ASPECTS is the best predictor of clinical outcome in acute ischemic stroke: a retrospective, combined semi-quantitative and quantitative assessment. *PLoS One* 2016;11:e0147910 [CrossRef Medline](#)
- Dababneh H, Bashir A, Guerrero WR, et al. Mean transit time on Aquilion ONE and its utilization in patients undergoing acute stroke intervention. *J Vasc Interv Neurol* 2014;7:73–81 [Medline](#)
- Eilaghi A, Brooks J, d'Esteire C, et al. Reperfusion is a stronger predictor of good clinical outcome than recanalization in ischemic stroke. *Radiology* 2013;269:240–48 [CrossRef Medline](#)
- Zhu G, Heit JJ, Martin BW, et al. Optimized combination of b values for IVIM perfusion imaging in acute ischemic stroke patients. *Clin Neuroradiol* 2020;30:535–44 [CrossRef Medline](#)
- Istratov AA, Vyvenko OF. Exponential analysis in physical phenomena. *Rev Sci Instrum* 1999;70:1233–57 [CrossRef](#)
- Le Bihan D, Turner R. The capillary network: a link between IVIM and classical perfusion. *Magn Reson Med* 1992;27:171–78 [CrossRef Medline](#)
- Sorensen AG, Copen WA, Ostergaard L, et al. Hyperacute stroke: simultaneous measurement of relative cerebral blood volume, relative cerebral blood flow, and mean tissue transit time. *Radiology* 1999;210:519–27 [CrossRef Medline](#)
- Sakoh M, Röhl L, Gyldensted C, et al. Cerebral blood flow and blood volume measured by magnetic resonance imaging bolus tracking after acute stroke in pigs. *Stroke* 2000;31:1958–64 [CrossRef Medline](#)
- Federau C, Hagmann P, Maeder P, et al. Dependence of brain intravoxel incoherent motion perfusion parameters on the cardiac cycle. *PLoS One* 2013;8:e72856 [CrossRef Medline](#)
- Fiebach JB, Jansen O, Schellinger PD, et al. Serial analysis of the apparent diffusion coefficient time course in human stroke. *Neuroradiology* 2002;44:294–98 [CrossRef Medline](#)
- Federau C, O'Brien K, Meuli R, et al. Measuring brain perfusion with intravoxel incoherent motion (IVIM): initial clinical experience. *J Magn Reson Imaging* 2014;39:624–32 [CrossRef Medline](#)
- Iima M, Partridge SC, Le Bihan D. Six DWI questions you always wanted to know but were afraid to ask: clinical relevance for breast diffusion MRI. *Eur Radiol* 2020;30:2561–70 [CrossRef Medline](#)